REPORT DOCUMENTATION PAGE

Form Approved OMB No. 0704-0188

1. REPORT DATE *(DD-MM-YYYY)*	2. REPORT TYPE	3. DATES COVERED *(From – To)*
14-12-2004	Final Report	1 November 2003 - 28-Dec-05

4. TITLE AND SUBTITLE

Porous Semiconductor Growth

5a. CONTRACT NUMBER
FA8655-03-1-3070

5b. GRANT NUMBER

5c. PROGRAM ELEMENT NUMBER

6. AUTHOR(S)

Professor Asim K Ray

5d. PROJECT NUMBER

5d. TASK NUMBER

5e. WORK UNIT NUMBER

7. PERFORMING ORGANIZATION NAME(S) AND ADDRESS(ES)
Queen Mary, University of London
Mile End Road
Department of Materials
London E1 4NS
United Kingdom

8. PERFORMING ORGANIZATION REPORT NUMBER

N/A

9. SPONSORING/MONITORING AGENCY NAME(S) AND ADDRESS(ES)

EOARD
PSC 802 BOX 14
FPO 09499-0014

10. SPONSOR/MONITOR'S ACRONYM(S)

11. SPONSOR/MONITOR'S REPORT NUMBER(S)
SPC 03-3070

12. DISTRIBUTION/AVAILABILITY STATEMENT

Approved for public release; distribution is unlimited.

13. SUPPLEMENTARY NOTES

14. ABSTRACT

This report results from a contract tasking Queen Mary, University of London as follows: The Grantee will investigate fabrication and analysis of Cadmium Sulphide (CdS) nanowires grown by depositing CdS nanoparticles in porous silicon and alumina.

15. SUBJECT TERMS
EOARD, Quantum Dots, Semiconductor Growth, Calmium Sulfide

16. SECURITY CLASSIFICATION OF:			17. LIMITATION OF ABSTRACT	18, NUMBER OF PAGES	19a. NAME OF RESPONSIBLE PERSON
a. REPORT	b. ABSTRACT	c. THIS PAGE			KEVIN J LAROCHELLE, Maj, USAF
UNCLAS	UNCLAS	UNCLAS	UL	16	**19b. TELEPHONE NUMBER** *(Include area code)* +44 (0)20 7514 3154

FINAL REPORT

November 2003 –October 2004

Author: Professor Asim K Ray

CONTENTS

1.0 ESSENTIAL INFORMATION

Project title:	Porous Semiconductor Growth
EOARD Grant No:	033070
Value of the project:	$20,000
Project Supervisor:	Dr. Ashwani K. Sharma Space Vehicles Directorate Air Force Research Laboratory 3550 Aberdeen Avenue SE Kirtland AFB NM 87117 *ashwani.sharma@kirtland.af.mil*
Academic Supervisor:	Professor Asim K Ray School of Engineering Sheffield Hallam University, Sheffield S1 1WB a.k.ray@shu.ac.uk
EOARD Program Manager:	Dr. Donald Smith European Office of Aerospace Research and Development (EOARD) 223/231 Old Marylebone Road London NW1 5TH sandy.smith@london.af.mil
Project students:	Mr. Anirban Bandyopadhyay Mr. Basudev Pradhan
Collaborators:	Dr. Aseel K Hassan School of Engineering Sheffield Hallam University, Sheffield S1 1WB a.hassan@shu.ac.uk Dr. Saiful I. Khondaker Center for Nano-& Molecular Science and Technology The University of Texas at Austin 1 University Station, A5300 saiful@mail.utexas.edu

2.0 SUMMARY OF ACHIEVEMENTS

2.1 Micropatterning through reverse self-assembly using photolithographically produced templates

Selective self-assembly properties of the thio and methoxy functional groups are utilised to micropattern (3-mercaptopropyl) trimethoxysilane molecules on the gold coated glass target starting with a nano-structured silicon grating template. Further modifications of the target surface are introduced by self-assembled monolayer of mercaptoacetic acid sodium salt molecules. The anisotropy in reflection properties is observed from the spectroscopic ellipsometric measurements in relation to the orientation of the plane of incidence. Conformations of spun adenine base and zinc oxide nanocomposite films on the gold substrate are found to depend upon its surface modifications due to the self-assembled monolayer.

2.2 **Development of neural network of DNA nanocomposites**

Interconnecting networks are fabricated by using calf-thymus DNA sodium salt and elementary DNA base adenine. Calf-thymus DNA sodium salt forms a complex wire-like network with poly(allylamine hydrochloride) which is a weak polyelectrolyte. The interconnection is formed by electrostatic forces during self-assembly. Adenine base and zinc oxide (ZnO) form a neural network the conformation of which depends on the molar ratio of the two ingredients. Electron tunnelling is responsible for conduction through the network involving calf-thymus DNA with no definite relation to applied voltage increment while adenine based network shows staircase behaviour with a 50mV step resembling single electron tunnelling through the nanogap.

2.3 Nanocrystalline CdS thin films prepared by chemical bath deposition method

Cadmium sulphide (CdS) thin films were prepared by the chemical bath (CB) deposition using a mixed aqueous solution of cadmium chloride, thiourea, and ammonium chloride. Thin films thickness in order of 66 nm film was characterised by X-Ray diffraction (XRD) pattern and Atomic force microscopy (AFM). The XRD patterns show that the CdS films are of hexagonal phase with preferred (002) orientation. The films are homogeneous over the coated surface. Band gap of E_g=2.4eV was calculated from both ellipsometry and absorbance.

2.4 Large photocurrent response of the Hybrid inorganic-polymer photodetector

We have studied the photocurrent responses of the hybrid inorganic-polymer device structure. CdS nanoparticles were used as inorganic photosensitive n-type materials and poly (9-vinayl carbazole) as a hole conducting polymer. This device behaves like a perfect diode in the dark condition with rectifying ratio and gives the large photocurrent response. The photo responsively increased due to the increased of the

reverse bias voltage. The topical value of the photocurrent responsivity is nearly 1.17(A/W) in minus 2 volt which is much higher than the GaN or other photodetectors.

2.5 Silver selenide nanocrystals in sol-gel derived titania matrix

We have made a comparative study on tuning of electronic property via doping with low band gap nanocrytaline material into nanocrystalline high band gap material. Titanium di-oxide (TiO_2, band gap 3.2eV) were prepared by sol-gel method and pre synthesised silver selenide (Ag_2Se_3, band gap 1.2eV) nanocomposites were incorporated into the matrix during the hydrolysis. The effect of incorporation of dopants into the sol-gel matrix were evaluated by X ray analysis and AFM, SEM. Sandwiched thin film of pristine and doped matrix (50nm) between ITO and Al electrodes have shown change in DC conductivity by two orders in magnitude. Apart from its significant changes in AC conductivity; the doped matrix shows dramatic transition in electronic behaviour from 200K to 225K which is reflected in its dipole moment distribution in the matrix. These phenomena presumably originated from titania matrix resulted in significant change in inter-cluster hopping and modulation in carrier transport modulation.

2.6 Use of DNA in Solid state Dye Sensitized Solar Cells

Calf-Thymus DNA and Adenine were used as solid state electrolyte in a dye sensitized nanocrystalline TiO_2 solar cell, where the sensitizing dye is Rose Bengal. Our studies have shown that short circuit current is increased from non-DNA based solar cell by 400%. The open circuit voltages are 580mV, 360mV and 280mV for non-DNA, adenine and Calf-Thymus DNA based structures, respectively. Our study on charge transfer phenomena between Rose Bengal and DNA's shows that a different CT band appears and this band contributes to the incident photon to electron conversion in the outer circuit. Impedance spectroscopic studies have shown that the incorporation of DNA into the device is affects the Fermi level matching with back electrode which lowers the effective barrier height. This resulted in lowering of open circuit voltage. Our work set a generalized example of using DNA molecules as a hole conducting materials which can recharge the electron deficient dye molecules for applications in photonics.

3.0 SCIENTIFIC NARRATIONS

3.1 CdS nanoparticles: preparation, characterisation and device applications

Microscopic glass slides and p-type silicon (100) $305\,\mu m$ thick having the resistivity of $0.05\,\Omega.m$ were used as substrates for the deposition of CdS films. Prior to deposition, glass slides and Si substrates were ultrasonically cleaned using propanol for 10 min, and then Millipore water for further 10 min, and finally dried in the oxygen-free Nitrogen gas flow. Solutions of 0.02M cadmium chloride ($CdCl_2$), 0.05M ammonium chloride (NH_4Cl) in 50ml milli-Q water (~18 MΩ) were prepared in a clean beaker. 0.4M ammonia ($NH_3.H_20$) was then added as a complexing agent to the beaker and the pH of the solution was maintained at the value of about 8.75. For film deposition, the substrates were kept inside the beaker containing the solution. The beaker was placed inside a water bath which was heated using a temperature- controlled hot plate with the magnetic stirrer in continuous operation to ensure homogeneous distribution of the chemicals. 0.05M thiourea ($(NH_2)_2CS$) solution was heated separately and added to the beaker which will initiate the CdS formation. The bath temperature was kept at $85 \pm 3\ ^{o}C$ for the duration of the deposition. The possible chemical reaction is shown below[1]:

$$CdCl_2 + (NH_2)_2CS + 2OH^- \longrightarrow CdS + H_2CN_2 + 2Cl^- + 2H_2O$$

The growth of the CdS film occurs either by ion-by-ion condensation of Cd and S ions on the substrate surface or due to adsorption of colloidal particles of CdS[2]. The solution was initially colourless, then it gradually changed colour to light yellow, then gold and then bright orange during the deposition. After 20 minutes of film deposition, the coated substrates were sonicated thoroughly in Millipore water in order to remove any loosely adhering powder. Finally samples were blown dry using N_2 gas and kept in a glass desiccator for at least 24 hours. CdS films deposited onto the microscopic glass substrates were used for optical measurements, while those deposited onto Si-substrates were used to perform spectroscopic ellipsometry (SE) study.

---

[1] R. Grecu, E. J. Popovici, M. Lădar, L. Pascu, E. Indrea, *J. optoelectron.adv.Mater*, 69 (2004) 127.

[2] P.J.Sebastian, H. Hu, *Adv. Mater. Opt. Electron.* 4(1994)407.

Optical absorption spectra of CdS films deposited on glass substrates were measured using a Hitachi U-2000 UV/Visible double beam spectrometer in the spectral range $300 - 900$ nm. A Philips $PW-1710$, grazing angle X-ray Diffractometer was used to study the crystallanity of CdS films using a CuKα radiation source of wavelength $\lambda = 0.1540\,nm$. The incident angle was kept constant at 1.0^{o} throughout the experiment. The closeness between relative intensity of observed and standard peaks indicates that the film is hexagonal structure. The film structure is shown to exhibit (100), (002), (101), (110), and (200) lattice planes, all of them represent the hexagonal wurtzite CdS structure with highly preferential orientation in (002) plane[3].

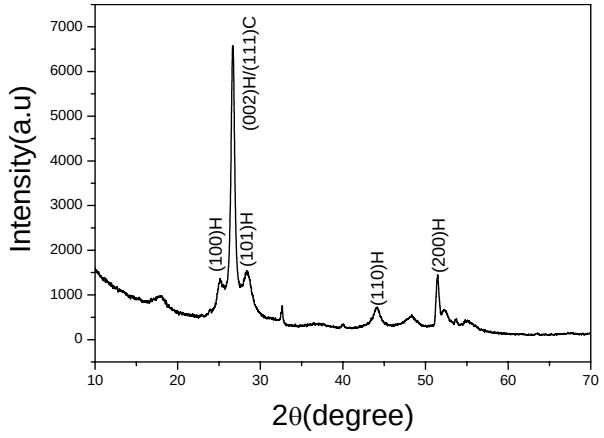

Figure1: XRD pattern of nanocrystalline films on silicon substrate

Spectroscopic ellipsometric measurements were performed with the angle of incidence fixed at the value of 70^{o}. The dedicated software is used for data acquisition and analysis. The measured ellipsometric parameters $\Psi(\lambda)$ and $\Delta(\lambda)$ are defined as the ratio of two complex reflection coefficients R_p and R_s for the p and s components of the polarised wave[4]:

$$\frac{R_p}{R_s} = \tan(\Psi)\exp(i\Delta) \qquad (1)$$

These two angles $\Psi(\lambda)$ and $\Delta(\lambda)$ indicate the polarisation change of the incident light wave as it is reflected at the different interfaces in the film. Measured $\Psi(\lambda)$ and $\Delta(\lambda)$ data are fitted to the CdS fitting model using point by point fitting procedure. This fitting procedure gives a thickness of CdS films of about 66 nm. This value was further confirmed by surface profilometer measurements.

[3] J.Zeng, J.Yang, Y. Zhu, Y.Liu, Y. Ian and H. Zheng, *Chem. Commun.*, 2001, 1332–1333

[4] X. Mathew, P.J. Sebastian, *Solar Energy Matter. solar Cells* 59 (1999) 85

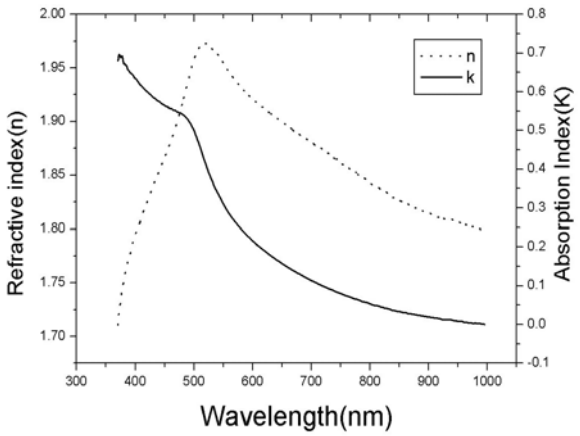

Figure 2: Dispersion relations of $n(\lambda)$ and $k(\lambda)$ obtained from spectroscopic ellipsometric measurements on CdS films

The optical band gap of the CdS films was calculated from both ellipsometry and absorption spectra by plotting $(\alpha h\nu)^2$ against hν and the resulting graphs were found to follow Tauc relation[5]

$$\alpha h\nu = A(h\nu - E_g)^n \qquad (2)$$

where $h\nu$ is the incident photon energy, α absorption coefficient, E_g the energy band gap, A is a constant, n=1/2 for the direct band gap semiconductor. The value of 2.4eV the energy band gap was determined from the extrapolated straight line to $(\alpha h\nu)^2$ =0 axis. The nature of the $(\alpha h\nu)^2$ against hν plot was different for measurements, possibly due to the film growth in different substrates.

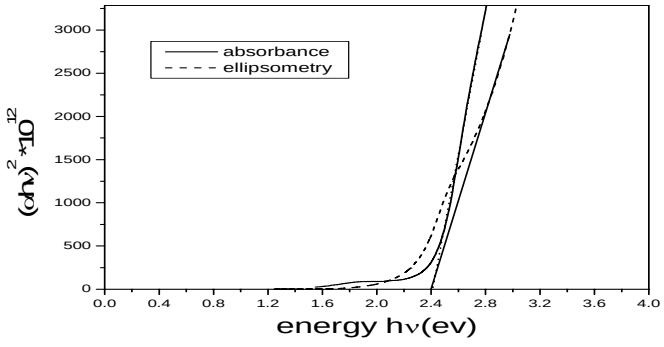

Figure 3: Tauc plots for CdS films

[5] J. Tauc(Ed.), Amorphous and Liquid Semiconductor, plenum Press, New York, 1974,159

Figure 4 shows a typical forward I(V) characteristic for a 60 nm thick CdS film sandwiched between ITO and Al contacts on logarithmic scales. The I(V) curve satisfies ohm's law for applied voltages $V < 0.4\,V$, whereas at higher applied voltages the characteristics shows a power law dependence of the form $I = \kappa V^n$, with a power index value of 2. The coefficient κ is a constant. Room temperature conductivity of the CdS films prepared by CBD is found to be in the region of $\sigma_{dc} = 10^{-3}\ S.m^{-1}$ which is agreement with published data.

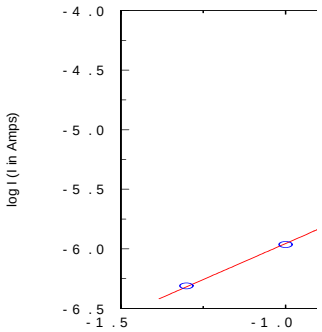

Figure 4: I(V) characteristic for ITO/CdS/Al structure

A 2mg/ml solution of poly(9-vinylcarbazole),brought from Aldrich chemical, in chloroform was prepared and then spin coated on the CdS coated ITO substrate with a spin speed of 2000rpm using the programmable spin coater. The thickness of the poly (9-vinylcarbazole) is about 50 nm. For the electrical characterisation electrode platinum (pt) was evaporated on the top of the ITO coated film from the tungsten filament boat at pressure less than 10^{-5} Torr. After the evaporation the effective cell dimension became 9mm length and 0.5mm width.

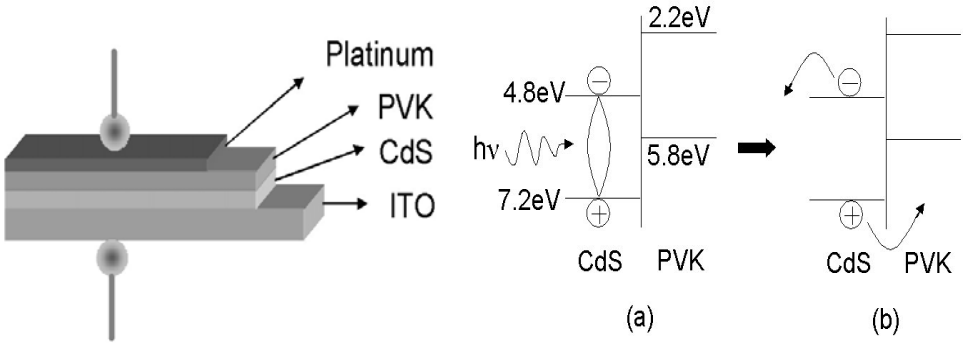

Figure 4: Device structure and energy band diagram

Current voltage characteristics were measured by Keithley 6517A electrometer in a microprocessor controlled measurement system. Light source was Bentham 605 solar

simulator fitted with Xenon lamp for general illumination; for monochromatic source SPEX 1683P broad band radiation source was fitted with SPEX 1681 0.22mm spectrometer for grating.

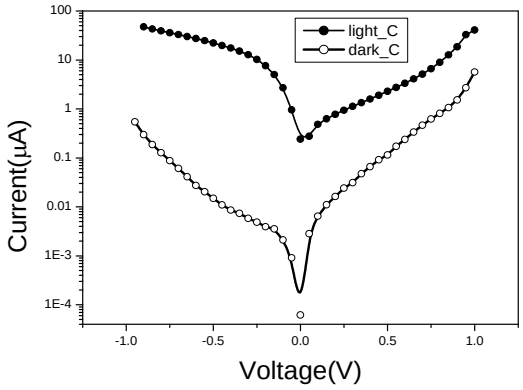

Figure 6: Current-voltage characteristics of ITO/CdS/Polymer diode

The current largely increased under the illumination of 100mw/cm^2 white light intensity than the dark current in 0.9 volt in reverse bias direction by a factor of about 160.

The inorganic-polymer p-n junction diode exhibits a high rectifying ratio. The photocurrent response of this device is much higher than other photodetector. The photocurrent responsivity of the device is bias dependent. The photocurrent spectrum is also similar to the absorbance spectra and the response is higher in the UV region. The photocurrent responsivity is nearly 1.17 in - 2 V which is much higher than the GaN or other photodetector

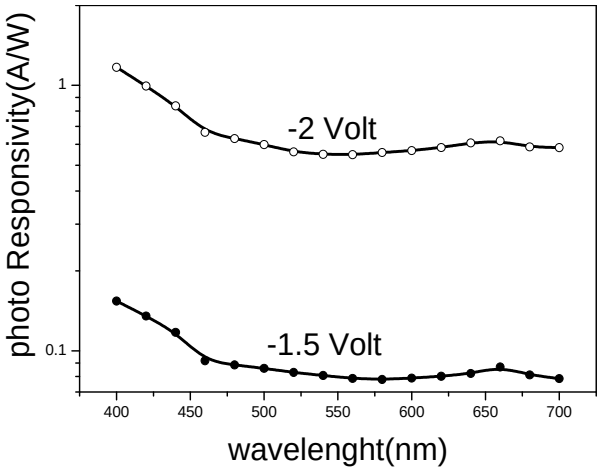

Figure 7: Photocurrent response of ITO/CdS/Polymer diode

3.2 Bandgap engineering by incorporation of nanoparticles in wideband materials

Absorbance spectra were taken for equilibrium hydrolysed solution before dip coating and also the solid thin film after transfer to the glass substrate. A red shift of the absorbance edge was observed after the addition of silver selenide. The band gap of doped materials was found to be lowered by $0.2eV$ in middle between pristine titanium oxide (3eV) and silver selenide (1.2eV). Elemental analysis was performed at different points of the doped sample and the ratio of count per second (cps) between Ti and O was found to vary from $1:2$ to $1:1.3$. This suggests that resulting sample is a mixed oxide composite, consisting of TiO_2, Ti_2O_3, and a trace of TiO. Si peak is due to the Si substrate on which films were grown for X-ray analysis. The AFM images indicated the presence of concentrated spots of diameter $\sim 25nm$. The percentage of silver in these concentrated regions varies by 60% in cps magnitude from those in the planar regions. The inclusion of silver selenide into the film of titanium oxides (Ti_xO_y) changes the DC conductivity by a factor of 10. Also the nature of conductivity is dramatically changed over the whole temperature range from 100K to 300K. While the pristine titania matrix shows a classical semiconducting behavior of increasing conductivity with the increasing temperature. This behavior is not modified largely with the voltage variation. But a sudden change in conductivity is observed nearly 200K, from which onwards rate of increase of conductivity with temperature exceeds rate of 0.1μS/K. This could be due to structural changes in the complex mixed oxides, which transforms semiconducting to metallic conducting sample. caused Unlike previous case, the nature of conductivity variation becomes sensitive to voltage variation after the addition of Ag_2Se_3 into the matrix.

4.0 Continuation of work on unique inorganic/organic nanocomposites for infrared quantum dot applications

The present proposal provides a technological innovation in nanoparticle science by generating a nanocomposite material consisting of PbS nanoparticles embedded in a matrix of phthalocyanine (Pc) molecules (see Figure 1). Hybrid inorganic-organic composites are an emerging class of new materials that hold significant promise. These nanostructured materials permit the design and engineering of functional systems for a wide range of applications. This is of particular interest in the development of nanoelectronic devices based on infra quantum dot effects. Lead sulphide (PbS) is a promising material, having a bandgap of 0.41 eV caused by a direct electron transition and a large Bohr radius of the exciton of about 18 nm. While humans may see in the visible spectral region, our ability to communicate information, detect and treat disease, harness new forms of energy and visualise threats to our safety and environments depend increasingly upon mastery of the infrared spectral region.

.

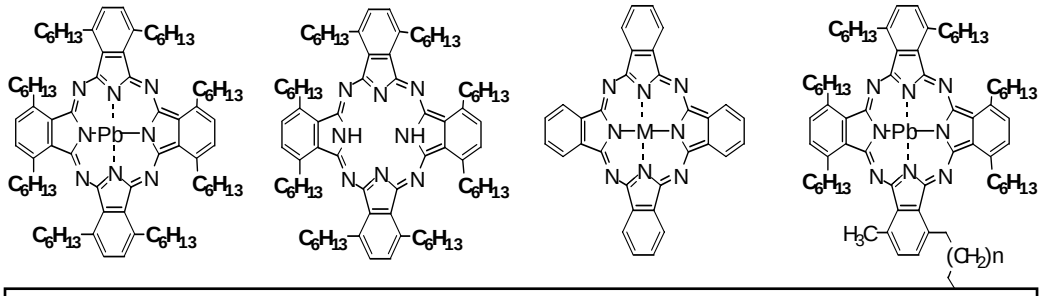

Figure 1: Chemical structure of Phthalocyanine

The science proposed in this application exploits a serendipitous finding by the PI that the Pb ion in certain lead phthalocyanine derivatives, eg compound (1), is released on exposure to H_2S gas to form the corresponding metal-free derivative (2) and PbS[6]. This conversion has been achieved in the solution phase and, more interestingly, on exposure of a spin coated film of (1) to H_2S gas. The latter result has recently been confirmed at the second partner laboratory as part of an unfunded preparative study for a joint research proposal. The UV/vis spectral changes showing the conversion of (1) into (2) on treatment with H_2S in the film formulation are shown in figure 2. The presence of PbS nanoparticles within the H_2S treated film has been demonstrated using a combination of TEM and energy dispersive x-ray analysis (EDXA) of an experiment conducted on a TEM grid as the support substrate. The TEM micrograph, figure 3, demonstrates the formation of ca. 2-5 nm size particles [with some evidence of nanoclusters contained within a matrix of (2)]. To our knowledge the composite we have developed is

[6] A.V. Nabok, A.K. Ray, M.J. Cook, P.M. Burnham, Iwantono, H. Yanuar, M. Simmonds and T.V. Basova , *IEEE Transactions on Nanotechnology, 3(3): 388- 394, 2004*

unprecedented and also unexpected; thus conventional thinking holds that removal of metal ions from the centre of the phthalocyanine by dilute acids is limited to rather few metallated derivatives, notably complexes containing two alkali metal ions, eg (**3**) M = Li,Li, or the divalent ions Mg^{2+} and Zn^{2+}. Indeed, again as part of the background study, we have shown that a film of another substituted phthalocyanine, tetra-t-butyl lead phthalocyanine, does *not* release lead on treatment with H_2S. Thus the finding that compound (**1**) behaves as described owes much to serendipity.

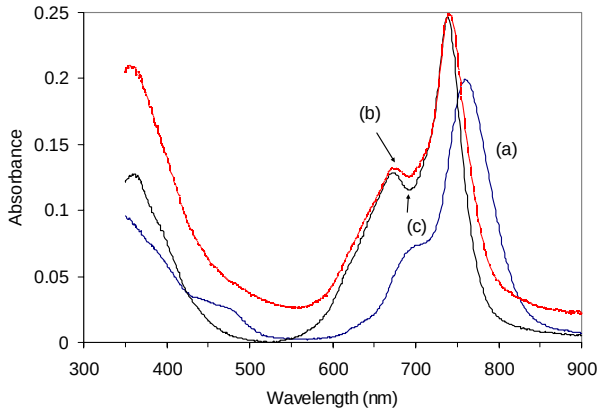

Figure 2 (left) - Spectra of (a) a spin coated film of (**1**); (b) after exposure to H_2S over 48 h to form (**2**); (c) an authentic film of (**2**).

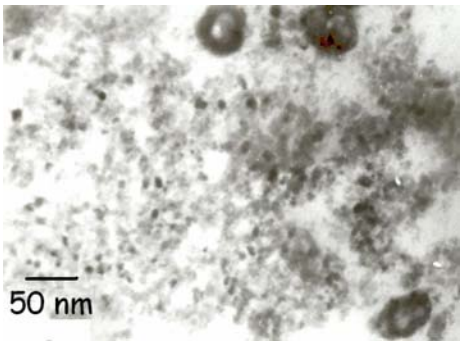

Figure 3 (left) - The TEM micrograph of a film of (**1**) after exposure to H_2S showing nanoparticles ca. 2-5 nm diameter and three ca. 50 nm clusters (at top and lower right of micrograph).

This project will explore the properties of formulations deemed to be most promising in terms of, for example, uniformity of particle size and distribution. The study of carrier transport through nanocomposite hybrid structures is of fundamental interest. The mechanism is strongly affected by the charge transfer between different phases within the material and energy level quantisation. A specially designed electrode system, figure 5, fabricated on a silicon substrate will be used for this purpose. The electrode assembly consists of two sets of 10 parallel electrodes each having electrode separation ~5-10nm. Steady state conduction through samples before and after H_2S treatment will be investigated at different temperatures ranging from liquid nitrogen to room temperature

both under dark and illuminated conditions. Measurement will provide physically meaningful information regarding the generation-recombination mechanism and the role of PbS nanoparticles. For particles with size in the order of 2 nm, as observed in our preliminary work, we would expect to observe Coulomb blockade phenomena in the room temperature I/V characteristics. This would be an important aspect for future investigations into developing nano technological devices. Capacitance voltage characteristics will be obtained to determine the location and type of potential barrier. Macroscopic measurements will also be undertaken in order to investigate charge carrier separation mechanisms in the PbS/phthalocyanine composites. The influence of annealing on the I-V characteristics will also be examined. The reverse breakdown voltage will be monitored in order to test the stability of the structure. Low frequency current and voltage noise measurements will be carried out on nanoparticle PbS films, providing quality assessment of nanocrystalline films. The knowledge of in-plane and through plane conductivity will be useful for determining the anisotropy in transport mechanism. It is worth pointing out that a collaborator of the PI has recently discovered that Pcs such as **(2)** easily and spontaneously align on suitable substrates.

Figure 5. AFM images of the electrodes

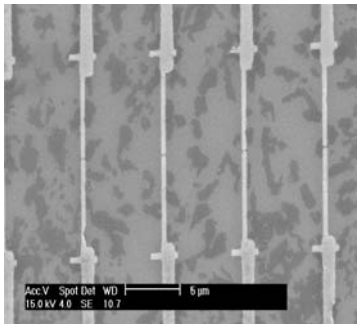

5.0 List of publications

1. A. Bandyopadhyay, A.K. Ray and A. Sharma, 2004 “Micropatterning through reverse self-assembly using photolithographically produced templates” *Nanotechnology* **15**,1603-1608.

2. A. Bandyopadhyay, A.K. Ray A. Sharma and S.I. Khondaker, “Transport through neural network of DNA nanocomposites” *IEEE Transactions on Nanotechnology (under review)*

3. B. Pradhan, A. Hassan, A.K. Sharma and A. K. Ray “Optical studies on nanocrystalline CdS thin films prepared by chemical bath deposition method” *J. NanoScience and Technology (submitted).*

4. **A. Bandyopadhyay, S. K. Batabyal, A.K. Ray and A. Sharma “Silver selenite in sol-gel derived titania matrix”** *Nanotechnolog.* (*under preparation*).

All papers contain the following acknowledgments:

This work is sponsored by the Air Force Office of Scientific Research, Air Force Material Command, USAF, under grant number FA8655-03-1-3070. The US Government is authorized to reproduce and distribute reprints for Government purpose notwithstanding any copyright notation thereon.

Appendices

1. PDF file of the reprint of publication:

   A. Bandyopadhyay, A.K. Ray and A. Sharma, 2004 “Micropatterning through reverse self-assembly using photolithographically produced templates” *Nanotechnology* **15**, 1603-1608.

2. Word document:

   A. Bandyopadhyay, A.K. Ray A. Sharma and S.I. Khondaker, “Transport through neural network of DNA nanocomposites” *IEEE Transactions on Nanotechnology (under review)*